

# Ghost Fano resonance in a double quantum dot molecule attached to leads

M. L. Ladrón de Guevara,<sup>1</sup> F. Claro,<sup>2</sup> and Pedro A. Orellana<sup>1</sup>

<sup>1</sup>*Departamento de Física, Universidad Católica del Norte, Casilla 1280, Antofagasta, Chile*

<sup>2</sup>*Facultad de Física, Pontificia Universidad Católica de Chile, Casilla 306, Santiago 22, Chile*

(Received 5 February 2003; published 30 May 2003)

We study the electronic transport through a double-quantum dot molecule attached to leads and examine the transition from a configuration in series to a symmetrical parallel geometry. We find that a progressive reduction of the tunneling through the antibonding state takes place as a result of the destructive quantum interference between different pathways through the molecule. The Fano resonance narrows down, disappearing entirely when the configuration is totally symmetric, so that only the bonding state participates in the transmission. In this limit, the antibonding state becomes completely localized.

DOI: 10.1103/PhysRevB.67.195335

PACS number(s): 73.21.La, 73.23.-b, 73.63.Kv

## I. INTRODUCTION

The tunneling of electrons through quantum dot structures has been the subject of active research during the past years. For the confinement of electrons in all the three dimensions, quantum dots are characterized by the discreteness of the energy levels, and for this reason, are often called “artificial atoms.”<sup>1,2</sup> One of the main features of transport through quantum dots is that the coherence of electrons is greatly preserved, as manifested in phenomena such as the Aharonov-Bohm oscillations in multiply connected geometries,<sup>3</sup> the Kondo effect in dots strongly coupled to electron reservoirs,<sup>4</sup> and Fano-type line shapes in transport through multiple channels.<sup>5</sup>

Two or more quantum dots can be coupled to form an “artificial molecule,” in which electrons are shared by different sites. The formation of bonding and antibonding states in such molecules has been studied by means of transport<sup>6-9</sup> as well as spectroscopy experiments.<sup>10,11</sup> Theoretical work on electron transport through serial quantum dot configurations is contained in Refs. 12, and quantum interference effects have been explored in parallel and “*T*-shaped” geometries.<sup>13-15</sup> Particular interest in quantum dot molecules lies in their potential application in quantum computing devices. In this context, diverse proposals have been made, where the quantum bits are built with electron-spin states<sup>16</sup> or with the coherent mode generated by discrete states in an artificial molecule.<sup>17</sup>

In this work, we study the electronic transport through a double-quantum dot molecule attached to leads, in a transition from a connection in series to a completely symmetrical parallel configuration. We examine the linear conductance at zero temperature and obtain the associated density of states of each of the dots. We find that the conductance spectrum is composed of a Lorentzian centered at the bonding energy, and a Fano line shape at the energy of the antibonding state. The latter arises due to the presence of a bound state of the molecule, immersed in the band continuum. A progressive line narrowing of the Fano peak is observed as the system transits from the series to the symmetrical parallel configuration. For the perfectly symmetrical geometry, the antibonding state is totally uncoupled of the leads, the bonding state becoming the only one that participates in the transmission.

In this extreme case, the antibonding state is localized, with zero localization length. Although exponentially localized states generally exist outside the band continuum, this state is in the conduction band and acts like a ghost of the Fano resonance.

## II. MODEL

We consider two neighboring quantum dots forming a molecule, coupled to left and right leads as shown in Fig. 1. Only one energy level in each dot is assumed relevant and the interdot and intradot electron-electron interactions are neglected. The system can be modeled by a noninteracting two-impurity Anderson Hamiltonian, which can be written as

$$H = H_m + H_l + H_r, \quad (1)$$

where  $H_m$  describes the dynamics of the isolate molecule,

$$H_m = \sum_{i=1}^2 \varepsilon_i d_i^\dagger d_i - t_c (d_2^\dagger d_1 + d_1^\dagger d_2). \quad (2)$$

Here  $\varepsilon_i$  is the energy of dot  $i$ ,  $d_i$  ( $d_i^\dagger$ ) annihilates (creates) an electron in dot  $i$ , and  $t_c$  is the interdot tunneling coupling.  $H_l$  is the Hamiltonian for the noninteracting electrons in the left and right leads,

$$H_l = \sum_{k_\alpha \in \{L,R\}} \varepsilon_{k_\alpha} c_{k_\alpha}^\dagger c_{k_\alpha}, \quad (3)$$

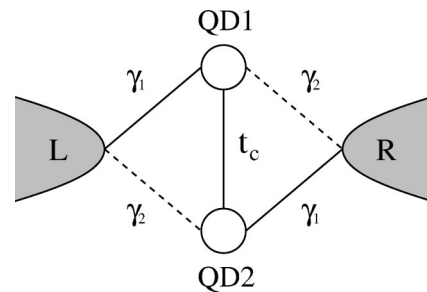


FIG. 1. Scheme of a quantum dot molecule coupled to left (L) and right (R) leads.

where  $c_{k_\alpha}$  ( $c_{k_\alpha}^\dagger$ ) is the annihilation (creation) operator of an electron of quantum number  $k_\alpha$  and energy  $\varepsilon_{k_\alpha}$  in the contact  $\alpha$ . Finally,  $H_I$  accounts for the tunneling between dots and leads,

$$H_I = \sum_{k_\alpha \in \{L,R\}} V_{1k_\alpha} d_1^\dagger c_{k_\alpha} + \text{H. c.} \\ + \sum_{k_\alpha \in \{L,R\}} V_{2k_\alpha} d_2^\dagger c_{k_\alpha} + \text{H. c.}, \quad (4)$$

with  $V_{ik_\alpha}$  being the tunneling matrix element. The linear conductance  $G$  is related to the transmission  $T(\varepsilon)$  of an electron of energy  $\varepsilon$  by the Landauer formula at zero temperature,<sup>18</sup>

$$G = \frac{2e^2}{h} T(\varepsilon_F). \quad (5)$$

To obtain  $G$  explicitly, we use the equation of motion approach for Green's function.<sup>18</sup> The retarded Green's function is defined by

$$G_{ij}^r(t) = -i\theta(t)\langle\{d_i(t), d_j^\dagger(0)\}\rangle, \quad i, j = 1, 2, \quad (6)$$

where  $\theta(t)$  is the step function. In the absence of interaction, the total transmission  $T(\varepsilon)$  can be expressed as

$$T(\varepsilon) = \text{tr}\{\mathbf{G}^a(\varepsilon)\mathbf{\Gamma}^R\mathbf{G}^r(\varepsilon)\mathbf{\Gamma}^L\}, \quad (7)$$

where  $\mathbf{G}^{r(a)}(\varepsilon)$  is the Fourier transform of the retarded (advanced) Green's function of the molecule, and the matrix  $\mathbf{\Gamma}^{L(R)}$  describes the tunneling coupling of the two quantum dots to the left (right) lead, with

$$\Gamma_{ij}^{L(R)} = 2\pi \sum_{k_{L(R)}} V_{ik_{L(R)}} V_{jk_{L(R)}}^* \delta(\varepsilon - \varepsilon_{k_{L(R)}}), \quad i, j = 1, 2. \quad (8)$$

The equation of motion method uses the Heisenberg equations for the Fermi operators of the molecule, which are inserted in the time derivatives of Green's functions of Eq. (6). This leads to first-order differential equations for  $G_{ij}^r$ 's, containing Green's functions for different dot operators as well as others involving dot and lead operators. Through the same procedure, equations for these new Green's functions are obtained, until having a closed set. A Fourier transform of such a set of equations takes it to an algebraic linear system for  $G_{ij}^r(\varepsilon)$ 's, the solution of which leads to the following expression for  $\mathbf{G}^r$ :

$$\mathbf{G}^r(\varepsilon) = \frac{1}{\Omega} \begin{pmatrix} \varepsilon - \varepsilon_2 + i\frac{\Gamma_{22}}{2} & -t_c + i\frac{\Gamma_{21}}{2} \\ -t_c + i\frac{\Gamma_{12}}{2} & \varepsilon - \varepsilon_1 + i\frac{\Gamma_{11}}{2} \end{pmatrix}, \quad (9)$$

where

$$\Omega = \left( \varepsilon - \varepsilon_1 + i\frac{\Gamma_{11}}{2} \right) \left( \varepsilon - \varepsilon_2 + i\frac{\Gamma_{22}}{2} \right) \\ - \left( -t_c + i\frac{\Gamma_{12}}{2} \right) \left( -t_c + i\frac{\Gamma_{21}}{2} \right), \quad (10)$$

with  $\Gamma_{ij} = \Gamma_{ij}^L + \Gamma_{ij}^R$ . A useful quantity that provides insight into the electronic distribution is the local density of states in dot  $i$ . It can be written in terms of the diagonal matrix elements of the retarded Green's function,

$$\rho_i(\varepsilon) = -\frac{1}{\pi} \text{Im}G_{ii}^r(\varepsilon), \quad i = 1, 2. \quad (11)$$

We are interested in the particular situation described in Fig. 1, in which  $\Gamma_{11}^R = \Gamma_{22}^L \equiv \gamma_1$  and  $\Gamma_{11}^L = \Gamma_{22}^R \equiv \gamma_2$ , so that  $\gamma_2 = 0$  represents a connection in series and  $\gamma_2 = \gamma_1$  represents a symmetrical configuration in parallel. For this case, the nondiagonal matrix elements of the matrices  $\mathbf{\Gamma}^{L,R}$  obey  $\Gamma_{21}^L = \Gamma_{12}^L = \Gamma_{21}^R = \Gamma_{12}^R \equiv \sqrt{\gamma_1\gamma_2}$ .

### III. CONDUCTANCE AND LOCAL DENSITY OF STATES

Introducing Eqs. (9) and (10) in Eq. (7) and then in (5), and using the above values of the  $\mathbf{\Gamma}^{L,R}$  matrix elements, we obtain the following expression for the conductance:

$$G(\varepsilon) = \frac{2e^2}{h} \frac{4}{C_1} [t_c \bar{\gamma} - \gamma_{12}(\varepsilon - \bar{\varepsilon})]^2, \quad (12)$$

where

$$C_1 = \left[ (\varepsilon - \bar{\varepsilon})^2 - (\Delta\varepsilon/2)^2 - t_c^2 - \frac{(\Delta\gamma)^2}{4} \right]^2 \\ + 4[\bar{\gamma}(\varepsilon - \bar{\varepsilon}) - t_c\gamma_{12}]^2, \quad (13)$$

with  $\bar{\varepsilon} = (\varepsilon_1 + \varepsilon_2)/2$ ,  $\Delta\varepsilon = \varepsilon_1 - \varepsilon_2$ ,  $\bar{\gamma} = (\gamma_1 + \gamma_2)/2$ ,  $\Delta\gamma = \gamma_1 - \gamma_2$ , and  $\gamma_{12} = \sqrt{\gamma_1\gamma_2}$ . The densities of states at each of the quantum dots are, in turn,

$$\rho_1(\varepsilon) = \frac{1}{\pi C_1} \left\{ \bar{\gamma} \left[ t_c^2 + \frac{(\Delta\gamma)^2}{4} + \left( \varepsilon - \bar{\varepsilon} + \frac{\Delta\varepsilon}{2} \right)^2 \right] \right. \\ \left. + 4t_c\gamma_{12} \left( \varepsilon - \bar{\varepsilon} + \frac{\Delta\varepsilon}{2} \right) \right\} \quad (14)$$

and

$$\rho_2(\varepsilon) = \frac{1}{\pi C_1} \left\{ \bar{\gamma} \left[ t_c^2 + \frac{(\Delta\gamma)^2}{4} + \left( \varepsilon - \bar{\varepsilon} - \frac{\Delta\varepsilon}{2} \right)^2 \right] \right. \\ \left. + 4t_c\gamma_{12} \left( \varepsilon - \bar{\varepsilon} - \frac{\Delta\varepsilon}{2} \right) \right\}, \quad (15)$$

with  $C_1$  being the same as Eq. (13).

First, let us consider the case with  $\Delta\varepsilon = 0$ . It follows from Eqs. (12) and (13) that  $G(\varepsilon)$  has two resonances, corresponding to the bonding and antibonding states, at the energies

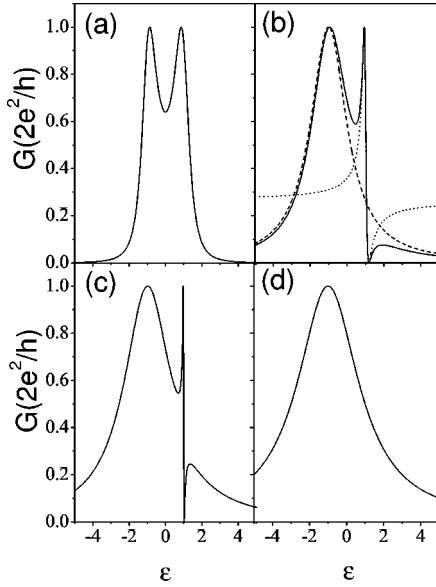


FIG. 2. Conductance as a function of the Fermi energy, for  $\Delta\varepsilon=0$ ,  $t_c=\gamma_1$  and different values of  $\gamma_2$ : (a)  $\gamma_2=0$ , (b)  $\gamma_2=0.3\gamma_1$ , (c)  $\gamma_2=0.6\gamma_1$ , and (d)  $\gamma_2=\gamma_1$ . The dash and dotted lines in (b) correspond, respectively, to the Breit-Wigner and Fano line shapes of Eqs. (19) and (20).

$$\varepsilon_{\pm} = \bar{\varepsilon} \pm \sqrt{t_c^2 - \frac{(\Delta\gamma)^2}{4}}, \quad (16)$$

which in general differ from the eigenvalues for the isolate molecule,  $\varepsilon_{\pm}^0 = \bar{\varepsilon} \pm t_c$ . The resonances can be distinguished only when  $|t_c| > |\Delta\gamma|/2$ , and the separation between them decreases as  $|\Delta\gamma|/2$  approaches  $|t_c|$ . Thus, the level of attraction produced by the connection to the leads becomes smaller as the coupling strength  $\gamma_2$  increases, up to vanishing when  $\gamma_2 = \gamma_1$ , where the bonding and antibonding states coincide with those of the isolated molecule. A similar level attraction is reported by Kubala *et al.* in Ref. 19 in an Aharonov-Bohm ring with a quantum dot in each of its arms.

We notice also that the conductance vanishes at the Fermi energy

$$\varepsilon_A = \bar{\varepsilon} + t_c \bar{\gamma} / \gamma_{12} \quad (17)$$

provided  $\gamma_2 \neq 0, \gamma_1$ . This antiresonancelike behavior, characterized by strictly zero transmission, is a consequence of destructive quantum interference between different pathways through the dots, and is not present for the connection in series, where only one possible pathway exists. Also, it can be shown that  $G(\varepsilon)$  reaches the quantum limit  $2e^2/h$  at specific values of the energy provided  $|t_c| \geq |\Delta\gamma|/2$ . For the molecule connected in series perfect transmission requires that the interdot coupling strength be at least  $\gamma_1/2$ , while in the parallel configuration with a weak interdot coupling it behaves as an ideal channel if the dot-lead coupling strengths are all of similar magnitude. Without loss of generality we can set  $\bar{\varepsilon}=0$ , a convention we adopt in what follows.

In Fig. 2 we have plotted the conductance as a function of the Fermi energy for  $\Delta\varepsilon=0$ ,  $t_c=\gamma_1$ , and different values of

$\gamma_2$ . For the configuration in series [Fig. 2(a)], the bonding and antibonding resonances are clearly resolved. For  $\gamma_2 \neq 0, \gamma_1$ , as in Figs. 2(b) and 2(c), the conductance exhibits the antiresonance mentioned above, and there is a progressive increase (reduction) of the width of the bonding (antibonding) resonance, as  $\gamma_2$  becomes larger ( $\gamma_2 < \gamma_1$ ). When  $\gamma_2 = \gamma_1$  [Fig. 2(d)] the antiresonance and the peak associated to the antibonding state are no longer present.

It can be shown that the conductance for  $\Delta\varepsilon=0$  is composed by a Breit-Wigner and a Fano line shape centered at the bonding and antibonding energies, respectively. Defining the quantities  $\Gamma_-$  and  $\Gamma_+$  by

$$\Gamma_{\pm} = \bar{\gamma} \pm \gamma_{12}, \quad (18)$$

in the limit  $\Gamma_+ \gg \Gamma_-$  and around  $\varepsilon = -t_c$ ,  $G(\varepsilon)$  can be approximated by

$$G(\varepsilon) \approx \frac{2e^2}{h} \frac{\Gamma_+^2}{\Gamma_+^2 + (\varepsilon + t_c)^2}, \quad (19)$$

and around  $\varepsilon = t_c$ , by the Fano line shape of width  $\Gamma_-$

$$G(\varepsilon) \approx \frac{2e^2}{h} \frac{\Gamma_+^2}{\Gamma_+^2 + 4t_c^2} \frac{(Q + e_-)^2}{1 + e_-^2}, \quad (20)$$

where  $Q = -2t_c/\Gamma_+$  and  $e_- = (\varepsilon - t_c)/\Gamma_-$  ( $\Gamma_- \neq 0$ ). The width of the bonding resonance  $\Gamma_+$  ranges from  $\gamma_1/2$  for the connection in series to  $2\gamma_1$  in the symmetrical case, while  $\Gamma_-$  decreases from  $\gamma_1/2$  to become infinitely small when  $\gamma_2$  approaches  $\gamma_1$ . A similar line reduction in the conductance spectrum is discussed in Ref. 20 in a junction with two resonant impurities. This line narrowing (widening) in the conductance can be interpreted as an increase (reduction) of the lifetime  $\tau = \hbar/\Gamma$  of the corresponding molecular state, with  $\Gamma$  being the associated linewidth. The strong narrowing of the Fano peak when  $\gamma_2$  is close to  $\gamma_1$  is a signal of slow transitions between the antibonding state and the leads. The lifetime of the antibonding state becomes infinitely long when  $\gamma_2$  approaches  $\gamma_1$ . Typically, the  $\gamma$ 's are of the order of meV's, so that the lifetimes of quantum dots attached to leads in series are of the order of *picoseconds*. However, if in the present configuration  $\gamma_1 = 10$  meV and  $\gamma_2 = 9.9$  meV, one obtains  $\Gamma_- = 5.5 \times 10^{-4}$  meV, then the lifetime of the antibonding state is  $\tau_- \approx 33$  ns, that is, four orders of magnitude larger. It is interesting to note that, as follows from expressions (12) and (13) and as displayed by Fig. 2(d), when  $\gamma_2 = \gamma_1$ , the Fano resonance entirely disappears and the conductance reduces exactly to the Lorentzian

$$G(\varepsilon) = \frac{2e^2}{h} \frac{4\gamma_1^2}{(\varepsilon + t_c)^2 + 4\gamma_1^2}, \quad (21)$$

expression with the form of the conductance of a single-quantum dot centered at the bonding energy, with an effective line broadening  $\gamma_e = 2\gamma_1$ . This would indicate that only the bonding state contributes to the transmission through the molecule.

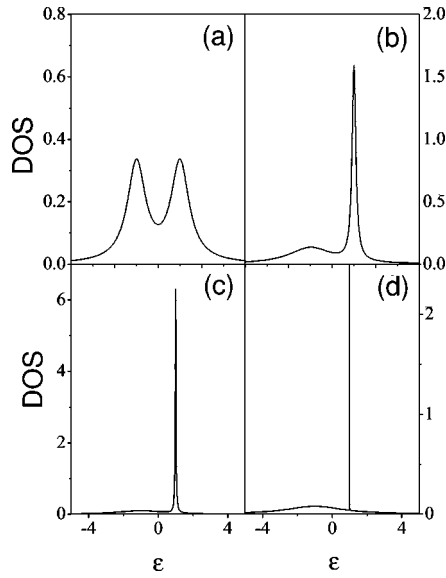


FIG. 3. Density of states  $\rho$  as a function of the Fermi energy, for  $\Delta\varepsilon=0$ ,  $t_c=\gamma_1$  and different values of  $\gamma_2$ : (a)  $\gamma_2=0$ , (b)  $\gamma_2=0.3\gamma_1$ , (c)  $\gamma_2=0.6\gamma_1$ , and (d)  $\gamma_2=\gamma_1$ .

Additional insight into the physics underlying these results can be obtained by examining the local density of states in each of the quantum dots. For  $\Delta\varepsilon=0$ , the density of states at both quantum dots is the same, and the electron has the same probability of being found at one or the other (covalent limit). It is straightforward to show that  $\rho_{1,2}=\rho$  is a superposition of two Lorentzians of widths  $\Gamma_+$  and  $\Gamma_-$  at the bonding and antibonding energies, respectively,

$$\rho(\varepsilon) = \frac{1}{2\pi} \left[ \frac{\Gamma_+}{(\varepsilon+t_c)^2 + \Gamma_+^2} + \frac{\Gamma_-}{(\varepsilon-t_c)^2 + \Gamma_-^2} \right]. \quad (22)$$

Figure 3 shows this quantity as a function of the energy for the same parameters used in Fig. 2. As we see, the local density of states is the simple superposition of two Lorentzians, one wide and one narrow as one approaches the symmetric configuration. For  $\gamma_2=\gamma_1$ , the Lorentzian centered at the bonding energy acquires the width  $2\gamma_1$ , while that at the antibonding energy becomes a  $\delta$  function. This last result indicates that the antibonding state turns totally localized in the molecule. In fact, it is straightforward to show that the Green function of this state ( $G_{aa}^r(t) = -i\theta(t)\langle\{d_a(t), d_a^\dagger(0)\}\rangle$ , where  $d_a=(d_1-d_2)/\sqrt{2}$ ) obeys the equation of motion of an isolated state.

Now, let us discuss how a finite difference in the energies of the different quantum dots modifies the results found in the fully symmetrical situation. When  $\varepsilon_1 \neq \varepsilon_2$  and  $\gamma_2=\gamma_1$ , the conductance takes the form

$$G(\varepsilon) = \frac{2e^2}{h} \frac{4\gamma_1^2(t_c - \varepsilon)^2}{C_2} \quad (23)$$

with

$$C_2 = \left[ \left( \frac{\Delta\varepsilon}{2} \right)^2 + (t_c - \varepsilon)(t_c + \varepsilon) \right]^2 + 4\gamma_1^2(t_c - \varepsilon)^2. \quad (24)$$

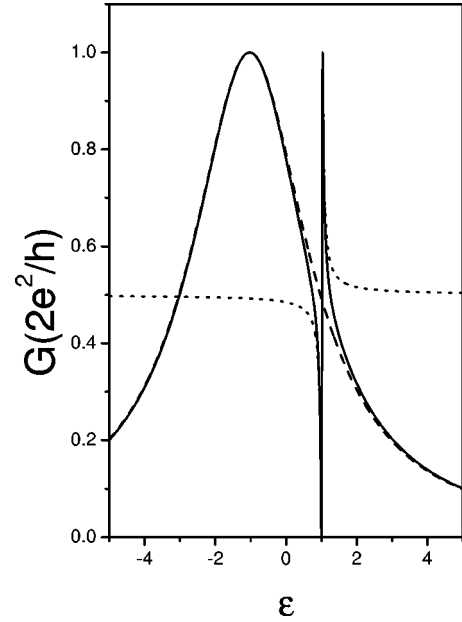


FIG. 4. Conductance as a function of the Fermi energy, for  $\Delta\varepsilon=\gamma_1/2$ ,  $t_c=\gamma_1$ , and  $\gamma_2=\gamma_1$ . The dash and dotted lines are the Lorentzian and the Fano line shape of Eqs. (26) and (26), respectively.

Now the antiresonance takes place in  $\varepsilon_A=t_c$  and the resonances are further apart than for  $\Delta\varepsilon=0$ , as one would expect, with their positions depending quadratically on  $\Delta\varepsilon$ . As before, the conductance is a convolution of a Lorentzian at the bonding energy and a Fano line shape at the antibonding energy. For  $\Delta\varepsilon \lesssim t_c$  the Lorentzian has a constant line broadening  $2\gamma_1$ ,

$$G(\varepsilon) \approx \frac{2e^2}{h} \frac{4\gamma_1^2}{(\varepsilon - \varepsilon_b)^2 + 4\gamma_1^2}, \quad (25)$$

with  $\varepsilon_b = -[t_c + (\Delta\varepsilon)^2/(8t_c)]$ . The Fano line shape has a width dependent on the difference of energies of the quantum dots levels,  $\Gamma_a = \gamma_1(\Delta\varepsilon)^2/[8(t_c^2 + \gamma_1^2)]$ ,

$$G(\varepsilon) \approx \frac{2e^2}{h} \frac{\gamma_1^2}{\gamma_1^2 + t_c^2} \frac{(e_a + Q)^2}{1 + e_a^2}, \quad (26)$$

where  $e_a = [\varepsilon - t_c(1 + \Gamma_a/\gamma_1)]/\Gamma_a$  and  $Q = t_c/\gamma_1$ . Figure 4 shows the conductance for  $\Delta\varepsilon=\gamma_1/2$  and  $t_c=\gamma_1$ , together with the corresponding pure Breit-Wigner and Fano curves given by Eqs. (25) and (26). Notice that the line broadening of the Fano peak depends quadratically on the value of  $\Delta\varepsilon$ , but differences of energy  $\Delta\varepsilon$  of the order of  $\gamma_1$  result in Fano peaks narrow enough; for instance, if  $\Delta\varepsilon=\gamma_1=t_c$ ,  $\Gamma_a = \gamma_1/16 \ll \gamma_1$ .

The local densities of states  $\rho_1$  and  $\rho_2$  are, respectively,

$$\rho_1(\varepsilon) = \frac{1}{\pi} \frac{(\Delta\varepsilon - 2t_c + 2\varepsilon)^2}{4C_2}, \quad (27)$$

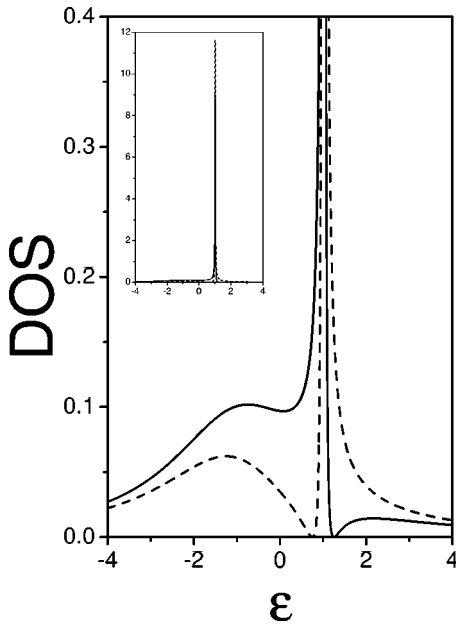


FIG. 5. Local densities of states  $\rho_1$  (solid line) and  $\rho_2$  (dash line) as a function of the Fermi energy, for  $\Delta\varepsilon = \gamma_1/2$ ,  $t_c = \gamma_1$ , and  $\gamma_2 = \gamma_1$ .

$$\rho_2(\varepsilon) = \frac{1}{\pi} \frac{(\Delta\varepsilon + 2t_c - 2\varepsilon)^2}{4C_2}, \quad (28)$$

and, as observed in Fig. 5, are the superposition of a Breit-Wigner resonance close to the bonding energy and a Fano line shape around the antibonding energy, similar to the conductance. It can be seen from the above analysis that for

quantum dots with different energies, both molecular states always contribute to the conductance.

#### IV. CONCLUSIONS

In this work, we studied the conductance and density of states at zero temperature of a quantum dot molecule attached to leads in the range between a connection in series and a symmetric parallel configuration. We found that the conductance is composed of Breit-Wigner and Fano line shapes at the bonding and antibonding energies, respectively, with their line broadenings controlled by the asymmetry of the configuration. The narrowing (widening) of a line in the conductance can be interpreted as an increase (reduction) of the lifetime of the corresponding molecular state. From the densities of states, it can be deduced that the antibonding state becomes progressively more localized as the asymmetry of the configuration is reduced. Surprisingly, when the configuration is completely symmetrical, the tunneling through the antibonding state is totally suppressed and the bonding state is the only one participating in the transmission. In this limit, the antibonding becomes a coherent localized state with zero localization length. The strong reduction of the decoherence processes exhibited by the present system may have applications in quantum computing.

#### ACKNOWLEDGMENTS

F.C. and M.L.L.d.G. were supported in part by Cátedra Presidencial en Ciencia. F.C. received support from FONDECYT, Grant No. 1020829. P. A. O. would like to acknowledge financial support from Milenio ICM P99-135-F and FONDECYT under Grant No. 1020269.

<sup>1</sup>M.A. Kastner, *Rev. Mod. Phys.* **64**, 849 (1992).

<sup>2</sup>P.L. McEuen, E.B. Foxman, U. Meirav, M.A. Kastner, Yigal Meir, Ned S. Wingreen, and S.J. Wind, *Phys. Rev. Lett.* **66**, 1926 (1991); R.C. Ashoori, H.L. Stormer, J.S. Weiner, L.N. Pfeiffer, K.W. Baldwin, and K.W. West, *ibid.* **71**, 613 (1993); P.L. McEuen, *Science* (Washington, DC, U.S.) **276**, 1729 (1997).

<sup>3</sup>A. Yacoby, M. Heiblum, D. Mahalu, and Hadas Shtrikman, *Phys. Rev. Lett.* **74**, 4047 (1995); R. Schuster, E. Buks, M. Heiblum, D. Mahalu, V. Umansky, and H. Shtrikman, *Nature* (London) **385**, 417 (1997); E. Buks, R. Schuster, M. Heiblum, D. Mahalu, V. Umansky, *ibid.* **391**, 871 (1998); Yang Ji, M. Heiblum, D. Sprinzak, D. Mahalu, and Hadas Shtrikman, *Science* (Washington, DC, U.S.) **290**, 779 (2000).

<sup>4</sup>D. Goldhaber-Gordon, J. Göres, M.A. Kastner, Hadas Shtrikman, D. Mahalu, and U. Meirav, *Phys. Rev. Lett.* **81**, 5225 (1998); Sara M. Cronenwett, Tjerk H. Oosterkamp, and Leo Kouwenhoven, *Science* (Washington, DC, U.S.) **281**, 540 (1998); W.G. van der Wiel, S. De Franceschi, T. Fujisawa, J.M. Elzerman, S. Tarucha, and L.P. Kouwenhoven, *ibid.* **289**, 2105 (2000).

<sup>5</sup>J. Göres, D. Goldhaber-Gordon, S. Heemeyer, M.A. Kastner, Hadas Shtrikman, D. Mahalu, and U. Meirav, *Phys. Rev. B* **62**, 2188 (2000); A.A. Clerk, X. Waintal, and P.W. Brouwer, *Phys. Rev. Lett.* **86**, 4636 (2001); Kensuke Kobayashi, Hisashi

Aikawa, Shingo Katsumoto, and Yasuhiro Iye, *ibid.* **88**, 256806 (2002).

<sup>6</sup>R.H. Blick, D. Pfannkuche, R.J. Haug, K.v. Klitzing, and K. Eberl, *Phys. Rev. Lett.* **80**, 4032 (1998).

<sup>7</sup>H. Jeong, A.M. Chang, and M.R. Melloch, *Science* (Washington, DC, U.S.) **293**, 2221 (2001).

<sup>8</sup>A.W. Holleitner, C.R. Decker, H. Qin, K. Eberl, and R.H. Blick, *Phys. Rev. Lett.* **87**, 256802 (2001).

<sup>9</sup>A.W. Holleitner, R.H. Blick, A.K. Hüttel, K. Eberl, and J.P. Kotthaus, *Science* (Washington, DC, U.S.) **297**, 70 (2002).

<sup>10</sup>G. Schedelbeck, W. Wegscheider, M. Bichler, and G. Abstreiter, *Science* (Washington, DC, U.S.) **278**, 1792 (1997).

<sup>11</sup>T.H. Oosterkamp, T. Fujisawa, W.G. van der Wiel, K. Ishibashi, R.V. Hijman, S. Tarucha, and Leo P. Kouwenhoven, *Nature* (London) **395**, 873 (1998).

<sup>12</sup>G. Klimeck, G. Chen, and S. Datta, *Phys. Rev. B* **50**, 2316 (1994); Cheng Niu, Li-jun Liu, and Tsung-han Lin, *ibid.* **51**, 5130 (1995); C.A. Stafford and S. DasSarma, *Phys. Rev. Lett.* **72**, 3590 (1994); A. Aharony, O. Entin-Wohlman, Y. Imry, and Y. Levinson, *Phys. Rev. B* **62**, 13 561 (2000); Pedro A. Orellana, G.A. Lara, and Enrique V. Anda, *ibid.* **65**, 155317 (2002).

<sup>13</sup>Tae-Suk Kim and S. Hershfield, *Phys. Rev. B* **63**, 245326 (2001); Y. Takazawa, Y. Imai, and N. Kawakami, *J. Phys. Soc. Jpn.* **71**, 2234 (2002).

- <sup>14</sup>Kicheon Kang and Sam Young Cho, cond-mat/0210009v1, Phys. Rev. B (to be published).
- <sup>15</sup>Daniel Boese, Walter Hofstetter, and Herbet Schoeller, Phys. Rev. B **66**, 125315 (2002).
- <sup>16</sup>D. Loss and D.P. DiVincenzo, Phys. Rev. A **57**, 120 (1998).
- <sup>17</sup>R.H. Blick, A.K. Hüttel, A.W. Holleitner, E. M. Höhberger, H. Qin, J. Kirschbaum, J. Weber, W. Wegscheider, M. Bichler, K. Eberl, and J.P. Hotthaus, Physica E (to be published).
- <sup>18</sup>Supriyo Datta, *Electronic Transport in Mesoscopic Systems* (Cambridge University Press, Cambridge, 1997).
- <sup>19</sup>Björn Kubala and Jürgen König, Phys. Rev. B **65**, 245301 (2002).
- <sup>20</sup>T.V. Shahbazyan and M.E. Raikh, Phys. Rev. B **49**, 17 123 (1994).